Discovery of 6-Aryl-7-alkoxyisoquinoline Inhibitors of IκB Kinase-β (IKK-β)

John A. Christopher,*,† Paul Bamborough,*,† Catherine Alder,† Amanda Campbell,† Geoffrey J. Cutler,‡ Kenneth Down,† Ahmed M. Hamadi,† Adrian M. Jolly,† Jeffrey K. Kerns,§ Fiona S. Lucas,† Geoffrey W. Mellor,‡ David D. Miller,† Mary A. Morse,† Kiritkant D. Pancholi,‡ William Rumsey,§ Yemisi E. Solanke,† and Rick Williamson†

GlaxoSmithKline R&D, Medicines Research Centre, Gunnels Wood Road, Stevenage, Hertfordshire, SG1 2NY, U.K., GlaxoSmithKline R&D, New Frontiers Science Park, Third Avenue, Harlow, Essex, CM19 5AW, U.K., and GlaxoSmithKline Inc., 709 Swedeland Road, King of Prussia, Pennsylvania 19406

Received January 7, 2009

The identification and progression of a potent and selective series of isoquinoline inhibitors of IκB kinase-β (IKK-β) are described. Hit-generation chemistry based on IKK-β active-site knowledge yielded a weakly potent but tractable chemotype that was rapidly progressed into a series with robust enzyme and cellular activity and significant selectivity over IKK-α.

Protein kinases catalyze the transfer of the γ-phosphate from ATP[a] to the side chain hydroxyl group of tyrosine, serine, or threonine residues of proteins involved in the regulation of diverse cellular functions. Aberrant kinase activity is implicated in many diseases and makes this target class attractive for the pharmaceutical industry.[1] The IκB kinase (IKK) family has been the subject of intense research, since these kinases are central regulators of NF-κB transcription factors, controlling gene expression in innate and adaptive immune responses.[2] Four kinases in this family have been identified based on sequence homology (IKK-α, -β, -ε and TBK1). The most widely studied family member to date is IKK-β which is ubiquitously expressed and mediates activation of NF-κB p50/RelA in response to proinflammatory stimuli such as tumor necrosis factor-α (TNF-α) and lipopolysaccharide (LPS). The role of this canonical NF-κB pathway is well documented in chronic inflammatory disease, and consequently identification of selective IKK-β inhibitors has been a particular goal for anti-inflammatory drug discovery.[2,3] More recently a nonredundant role for IKK-α has been elucidated, in mediating signal transduction from TNF receptor family members, such as costimulation receptors CD40 and BAFFR on B lymphocytes.[4] In addition recent publications have identified possible roles of the IKK family in control of the cell cycle through regulation of the mitotic kinase Aurora A, with IKK-β proposed to control its concentration and IKK-α its activity.[5−7] Such effects, if confirmed, will govern the utility of IKK inhibitors. The identification of isoform selective IKK inhibitors will provide pharmacological reagents to further address the differential role of these kinases in health and disease. The discovery and development of small-molecule inhibitors of IKK-family kinases represent a significant area of research, as described in a recent review of the patent literature by Lowinger and colleagues.[8]

We have previously disclosed 2-amino-3,5-diarylbenzamide inhibitors of IKK-β (e.g., **1**, Chart 1).[9] The sulfonamide moiety

Chart 1. IKK-β Inhibitor **1**[9]

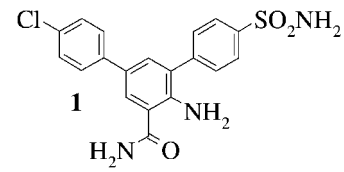

in **1** substantially enhanced IKK-β inhibitory potency, which we postulated was due to favorable hydrogen bonding interactions between the sulfonamide oxygens and either the Lys106 side-chain or the Asp103 backbone in the ATP-site of IKK-β. A hit generation array was designed to test the hypothesis that other scaffolds containing a sulfonamide feature would also be potent inhibitors of IKK-β. The strategy exploited tractable, one-step chemistry to build back toward the hinge area of the ATP site from meta- and para-substituted phenylsulfonamides. This strategy differs from the more common approach in which a core heterocycle acting as the hinge-binding group is modified by building out toward additional interactions. To select the hinge-binding groups, first a 3D database was built from over 8000 aromatic halides passing stringent substructural developability filters and reagent availability checks.[10,11] A 3D pharmacophore was built using the conserved interactions between a homology model of IKK-β and docked phenylcarboxamide inhibitors such as **1**.[11] These are illustrated in Figure 1. Features used in the pharmacophore model included a hydrogen-bond acceptor positioned close to the backbone NH of the hinge residue Cys99. In addition, atomic location constraints were positioned along the bond vector leading toward the phenylsulfonamide group of **1**. One of these was used to constrain the position of a bromo substituent, while the other was used to constrain the position of the linked aromatic carbon atom, as shown in Figure 1b. The pharmacophore was then applied to filter the database down to 289 halides. The products **4** and **5** between these halides and phenylsulfonamide boronic acids **2** and **3** (Scheme 1) were enumerated and docked into the homology model. Assessment of the docking scores and visual compatibility with the site contributed to a final selection of 140 aryl halides.[11]

The 140 chosen halides were coupled to boronic acids **2** and **3** under standard Suzuki−Miyaura coupling conditions as shown in Scheme 1. A total of 184 of the 280 target compounds were successfully obtained, an acceptable synthetic success rate of

* To whom correspondence should be addressed. For J.A.C.: phone, +44 (0)1438 763578; fax, +44 (0)1438 768232; e-mail, john@christopher257.fsnet.co.uk. For P.B.: phone, +44 (0)1438 763246; fax, +44 (0)1438 763352; e-mail, Paul.A.Bamborough@gsk.com.

† GlaxoSmithKline R&D, Hertfordshire.

‡ GlaxoSmithKline R&D, Essex.

§ GlaxoSmithKline Inc.

[a] Abbreviations: ATP, adenosine triphosphate; LPS, lipopolysaccharide; TNF-α, tumor necrosis factor-α; BAFFR, B-cell activating factor receptor; PBMC, peripheral blood mononuclear cells.

10.1021/jm9000117 CCC: $40.75
Published on Web 04/06/2009

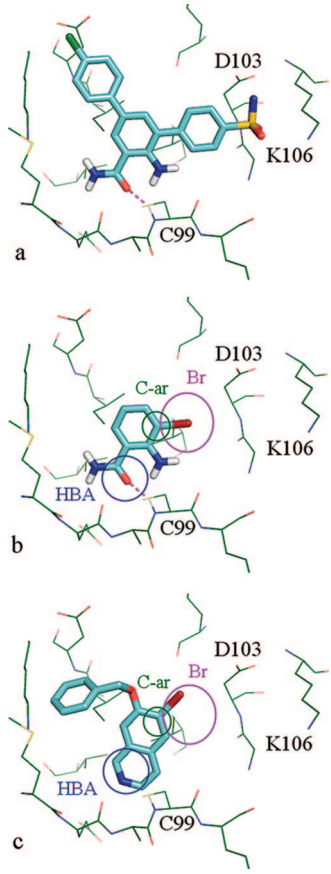

Figure 1. Pharmacophore based selection process for aryl halides: (a) **1** docked into IKK-β model; (b) positioning of H-bond acceptor, aromatic carbon, and bromo substituent pharmacophore features; (c) example pharmacophore search hit fitted to pharmacophore.

Chart 2. Isoquinoline Hits **6** and **7**

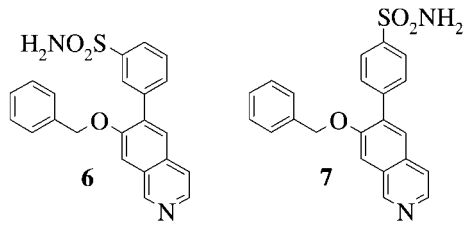

IKK-α $pIC_{50} < 4.6$ IKK-β pIC_{50} 5.1

IKK-α $pIC_{50} < 4.6$ IKK-β pIC_{50} 5.5

approximately 66% with coupling conditions that were not optimized specifically for this array. Products **4** and **5** were screened against a panel of tyrosine and serine/threonine kinases, including IKK-α and IKK-β. Isoquinolines **6** and **7** (Chart 2) were chosen for further evaluation and progression, primarily on the basis of their IKK-β activity, kinase selectivity profiles, and amenability to two-dimensional hit expansion.

Active compounds from the first iteration of chemistry described above were redocked into the ATP-binding site of a homology model of IKK-β, as illustrated in Figure 2 for **7**. As part of this, a more critical analysis of the binding modes predicted from the pharmacophore model was carried out. The binding mode consistent with the original pharmacophore-driven design hypothesis of the hit generation array, in which the sulfonamide group of **7** interacts with Asp103 and/or Lys106, looked improbable. It was apparent that in this binding mode the benzyloxy group would be poorly positioned in the back of

Scheme 1[a]

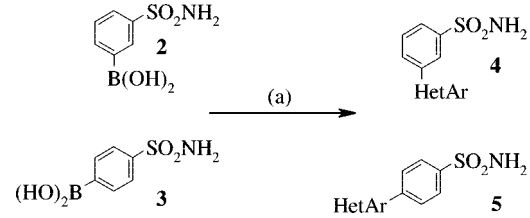

[a] Reagents and conditions: (a) heteroaryl halide, $PdCl_2$(dppf), 2 M (aq) Na_2CO_3, dioxane, water, 80 °C or microwave heating, 150 °C, 20 min.

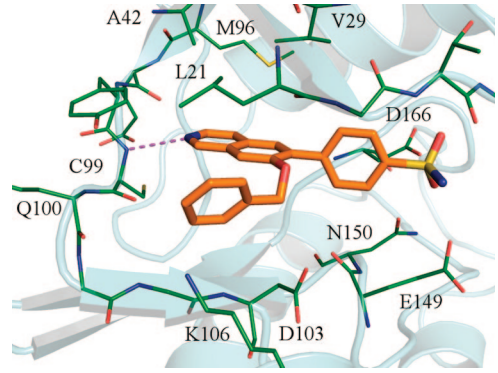

Figure 2. Model of IKK-β with docked **7**.

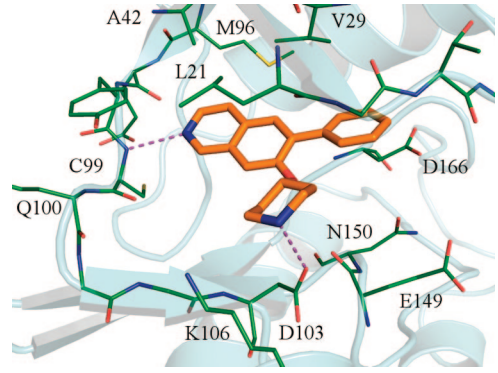

Figure 3. Model of IKK-β with docked compound **21**.

the ATP site, with strained torsion angles. In addition, burying a flexible linker in this way (as in Figure 1c) would be penalized entropically (see Figure 1c). A different binding mode appeared to be more plausible, in which the sulfonamide group lies at the back of the ATP site in the vicinity of Glu149 and Asp166 (Figure 2). In this orientation, the benzyloxy group projects toward the front of the site but makes no obvious favorable interactions other than steric contacts with Leu21 and Asp103. Comparison of the model of **7** with the predicted binding modes of other series such as **1**, combined with docking of multiple potential synthetic targets, led to the refined hypothesis that the 7-position benzyloxy group should optimally be replaced by O-linked 4-piperidine or 4-piperidine amides and sulfonamides, in combination with aryl groups at the 6-position. The hope was that this piperidine group would be positioned appropriately to interact with Asp103, as illustrated in Figure 3 for the docking of compound **21**.

To explore the template further, we required a robust, scalable route to the versatile key intermediate **14**, which would allow two-dimensional exploration of the template via O-alkylation and Suzuki−Miyaura coupling. Direct bromination of readily available 7-hydroxyisoquinoline (NBS, AcOH, room temp) efficiently resulted in selective bromination at the undesired

Scheme 2[a]

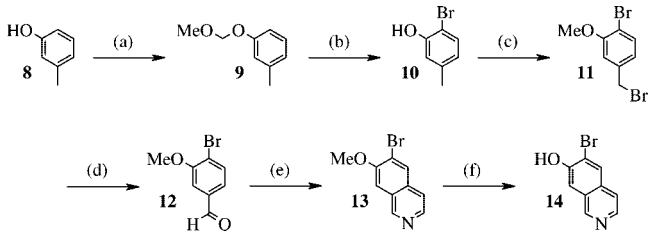

[a] Reagents and conditions: (a) dimethoxymethane, PTSA, CH_2Cl_2, Δ; (b) (i) *t*-BuLi, pentane, 0 °C, (ii) 1,2-dibromoethane, THF, −78°C, (iii) PTSA, MeOH, Δ; (c) (i) MeI, K_2CO_3, DMF, (ii) NBS, AIBN, CCl_4, Δ; (d) NaOEt, 2-nitropropane, EtOH, 90 °C; (e) (i) 2,2-dimethoxyethylamine, PhH, Δ, (ii) polyphosphoric acid, 85 °C; (f) LiI, pyridine, microwave heating, 175 °C.

8-position. An alternative route was utilized, starting from *m*-cresol **8** (Scheme 2). Methoxymethyl protection followed by ortho-lithiation, bromination, and O-deprotection yielded **10**. Reprotection of the phenol as the methyl ether was followed by radical bromination. The resulting benzyl bromide was converted to aldehyde **12** via the Hass−Bender procedure.[12] Condensation with 2,2-dimethoxyethylamine and polyphosphoric acid mediated cyclization of the resulting imine yielded **13**, which was deprotected with lithium iodide to provide **14**. Chemistry detailed in Scheme 3 was then employed to synthesize **16**−**28** from intermediate **14**, and compound **29** from 7-isoquinolinol. The inhibitory characteristics of **16**−**29** were assessed in IKK-α and IKK-β enzyme activity assays (Table 1). In line with **6** and **7**, selectivity was maintained for IKK-β over IKK-α (generally 10- to 100-fold). Substitution at the 6-position was favorable (compare **16**−**22** with **29**) with moderate to substantial increases in IKK-β potency being yielded by aryl groups or bromide at this position. Phenyl groups, unsubstituted or with para aminomethyl or sulfonamide substitution, yielded the greatest IKK-β potency (**21**, **20**, **17**, respectively). Homologation of the sulfonamide group (compare **17** to **18**) or moving the substituent to the meta position (compare **16** and **19** to **17** and **20**, respectively) was deleterious to the IKK-β potency and the selectivity over IKK-α. An initial exploration of piperidine N-substitution with acetyl (**24**−**26**) or ethanesulfonyl (**23**, **27**, **28**) groups indicated that substitution was tolerated in this position, albeit with at least a 10-fold drop in IKK-β potency. We attribute this loss of activity to the removal of the possibility of a charge−charge interaction between the piperidine nitrogen and Asp103. While this may not seem an exceptionally large decrease for such an interaction, it seems reasonable given the solvent exposure of the Asp103 side chain.

By use of chemistry analogous to that depicted in Scheme 3, **30**−**37** were prepared to probe the alkoxy substituent SAR further. Moving the ring nitrogen to the 3-position of the piperidine resulted in an approximately 10-fold drop-off in IKK-β potency (compare **30** and **32** to **21** and **17**, respectively, Table 2). The lower activity of **30** and **32** can be interpreted as resulting from the loss of the Asp103 interaction. Activity was largely restored by homologation (**31**, **33**), perhaps indicating that the additional methylene allows the Asp103 interaction to be restored. However, modeling predictions involving this part of the site are made challenging due to the abundance of H-bond accepting groups that could be involved in interactions with these protonated piperidines, including the backbone carbonyl and side chain acid of Glu149. Homologation in the 4-piperidine series resulted in a 10-fold loss of IKK-β potency (**34**, **35**). In line with our initial observations, sulfonylation of the piperidine nitrogen yielded only moderate IKK-β potency (**36**, **37**). Piperidine replacement by pyridine (**38**, **39**) was not profitable, with IKK-β potencies approximately 30- and 4-fold lower than the analogous saturated compounds **31** and **34**, indicating a preference for the more basic piperidine nitrogen.

The ability of key compounds to inhibit the production of TNF-α in lipopolysaccharide (LPS) stimulated peripheral blood mononuclear cells (PBMC) was investigated (Table 3). IKK-β enzyme potency translated into good to moderate PBMC efficacy, with a drop-off of typically less than 30-fold observed. Additionally, one of the most potent examples, **21**, showed very promising activity ($pIC_{50} = 5.9$) in an analogous human whole blood readout of TNF-α inhibition.

In addition to the highly encouraging IKK-β inhibitory characteristics of the compounds and selectivity within the IKK family against IKK-α, cross-screening of selected compounds against a panel of in-house kinases revealed an excellent overall profile. The exception is Rho kinase 1 (Rock1) where moderate selectivity (3- to 10-fold) was typical across the series. The subset of data shown in Table 4 is representative of a selective

Scheme 3[a]

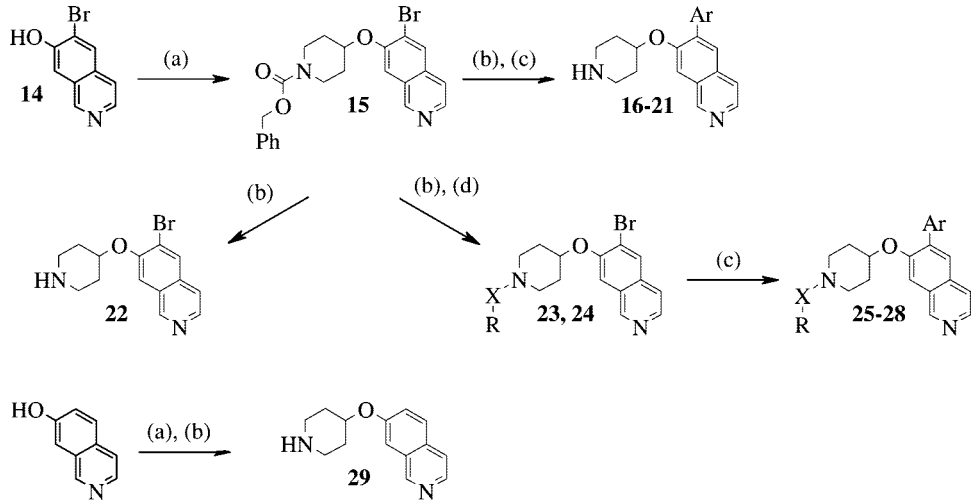

[a] Reagents and conditions: (a) 4-bromo-*N*-Cbz piperidine, K_2CO_3, DMF, 80 °C; (b) 4 M HCl/1,4-dioxane, microwave heating, 150 °C; (c) arylboronic acid, $PdCl_2$(dppf), 2 M (aq) Na_2CO_3, dioxane, water, microwave heating, 150 °C, 25 min; (d) Ac_2O, DIPEA, DMAP, CH_2Cl_2 or $EtSO_2Cl$, DIPEA, CH_2Cl_2.

Table 1. IKK-α and IKK-β Inhibition by Compounds **16**−**29**[a]

compd	Ar	-X-R	IKK-α pIC_{50}	IKK-β pIC_{50}
16	C_6H_4-3-SO_2NH_2	H	5.1	5.9
17	C_6H_4-4-SO_2NH_2	H	5.1	7.0
18	C_6H_4-4-$CH_2SO_2NH_2$	H	5.4	6.4
19	C_6H_4-3-CH_2NH_2	H	4.9	6.1
20	C_6H_4-4-CH_2NH_2	H	5.2	6.9
21	Ph	H	5.6	7.0
22	Br	H	5.0	6.4
23	Br	-SO_2Et	<4.6	5.3
24	Br	-C(O)Me	<4.6	4.9
25	Ph	-C(O)Me	4.8	5.5
26	C_6H_4-4-SO_2NH_2	-C(O)Me	<4.6	5.9
27	Ph	-SO_2Et	4.9	5.7
28	C_6H_4-4-SO_2NH_2	-SO_2Et	4.6	6.0
29	H	H	<4.6	5.3

[a] See Experimental Section for a description of assay conditions.

Table 2. IKK-α and IKK-β Inhibition by Compounds **30**−**39**[a]

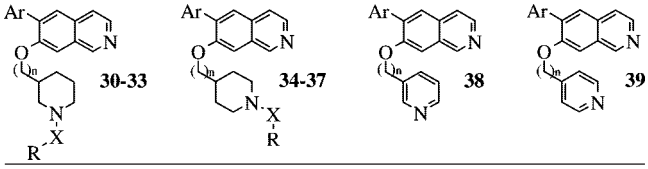

compd	6-substituent	*n*	-X-R	IKK-α pIC_{50}	IKK-β pIC_{50}
30	Ph	0	H	5.4	6.2
31	Ph	1	H	5.5	6.8
32	C_6H_4-4-SO_2NH_2	0	H	4.9	6.1
33	C_6H_4-4-SO_2NH_2	1	H	5.3	6.8
34	Ph	1	H	5.0	5.9
35	C_6H_4-4-SO_2NH_2	1	H	4.8	6.2
36	Ph	1	$SO_2(CH_2)_3NMe_2$	5.0	5.9
37	Ph	1	SO_2Et	4.7	5.6
38	Ph	1		<4.6	5.4
39	Ph	1		<4.6	5.3

[a] See Experimental Section for a description of assay conditions.

Table 3. Inhibition of TNF-α Production from LPS Stimulated PBMCs

compd	IKK-α pIC_{50}	IKK-β pIC_{50}	PBMC pIC_{50}
16	5.1	5.9	5.2
17	5.1	7.0	5.5
20	5.2	6.9	5.8
21	5.6	7.0	6.1
31	5.5	6.8	6.0
33	5.3	6.8	5.8
34	5.0	5.9	5.9

overall profile: for example, compound **21** showed $pIC_{50} < 6$ against all other 59 kinases tested. Lack of activity at p38α and MK2, kinases that could block LPS-induced TNF-α production, builds further confidence that the cellular activity observed with these compounds is mediated via IKK-β.

Conclusions

Hit-generation chemistry based on IKK-β active site knowledge gleaned from known inhibitor chemotypes led to the identification of **6** and **7**, which are moderately potent isoquinoline inhibitors of IKK-β. Initial explorations of substitution at the isoquinoline 6- and 7-positions led to a substantial enhancement in IKK-β enzyme potency, which translated into significant cellular activity. The series displays encouraging selectivity within the IKK family over IKK-α and across a wide variety of kinase enzyme and binding assays.

Experimental Section

General Experimental Procedures. Microwave reactions were performed in a Biotage Initiator 60 EXP microwave reactor. NMR spectra were obtained in the deuterated solvents indicated, on a Bruker DPX250, DPX400, or AV400 spectrometer referencing to tetramethylsilane for proton spectra. Exchangeable NH protons were not observed in the ^{1}H spectra of **17**−**19**, **22**, **40**, and **41**. Test compounds **6**, **7**, **16**−**39** possessed a purity of at least 95% as assessed by LCMS analysis. LCMS analysis was conducted on a Supelcosil LCABZ+PLUS column (3.3 cm × 4.6 mm i.d.), eluting with 0.1% formic acid and 0.01 M ammonium acetate in water (solvent A) and 0.05% formic acid and 5% water in acetonitrile (solvent B), using the following elution gradient: 0.0−0.7 min 0% B, 0.7−4.2 min 100% B, 4.2−4.6 min 100% B, 4.6−4.8 min 0% B at a flow rate of 3 mL/min. The mass spectra were recorded in electrospray positive and negative ion modes (ES +ve and ES −ve) on a Waters ZQ mass spectrometer. Accurate mass measurements were performed on Bruker Daltonics 7T FTICR-MS or Micromass Q-Tof 2 hybrid quadrupole mass spectrometers operating in electrospray positive ion mode.

General Procedure for the Preparation of 16−**22.** The procedure is exemplified by the preparation of **17** and **22**. Intermediate **15** (874 mg, 1.98 mmol) in 1,4-dioxane (2 mL) and HCl (4 M in 1,4-dioxane, 8 mL) was heated in a sealed vial in a microwave reactor at 150 °C for 15 min. After cooling and release of pressure (CAUTION), the mixture was concentrated in vacuo. The residue was triturated with Et_2O, and 6-bromo-7-(4-piperidinyloxy)isoquinoline (**22**, 639 mg, 1.68 mmol) was isolated as the dihydrochloride salt by filtration. ^{1}H NMR (400 MHz, MeOD) δ 9.62 (1H, s), 8.69 (1H, s), 8.50 (1H, d, J = 6.5 Hz), 8.36 (1H, d, J = 6.5 Hz), 8.13 (1H, s), 5.23−5.17 (1H, m), 3.51−3.31 (4H, m), 2.40−2.30 (2H, m), 2.20−2.19 (2H, m); LCMS (ES +ve) *m*/*z* 307.0, 309.1 $(M + H)^+$; HRMS (ES +ve) *m*/*z* found 307.04401 $(M + H)^+$, calcd for $C_{14}H_{16}BrN_2O$ 307.04405.

A mixture of 6-bromo-7-(4-piperidinyloxy)isoquinoline dihydrochloride (**22**, 40 mg, 0.11 mmol), 4-(4,4,5,5-tetramethyl-1,3,2-dioxaborolan-2-yl)benzenesulfonamide (35.7 mg, 0.13 mmol), dichloro(1,1′-bis(diphenylphosphino)ferrocene)palladium(II)−dichloromethane adduct (approximately 5 mg, 0.006 mmol), 2 M (aq) Na_2CO_3 (0.16 mL, 0.32 mmol) in water (0.14 mL), and 1,4-dioxane (0.30 mL) was heated in a sealed vial in a microwave reactor at 150 °C for 15 min. The mixture was passed through a 1 g SiO_2 cartridge, eluting with MeOH and then 5% NH_3 in MeOH. Purification by mass-directed HPLC followed by passage of product containing fractions through a 1 g polymer-supported aminopropyl cartridge eluting with MeOH yielded 4-[7-(4-piperidinyloxy)-6-isoquinolinyl]benzenesulfonamide (**17**, 17.5 mg, 0.05 mmol). ^{1}H NMR (400 MHz, DMSO-d_6) δ 9.19 (1H, s), 8.34 (1H, d, J = 5.6 Hz), 7.92 (1H, s), 7.86 (2H, d, J = 7.8 Hz), 7.76 (2H, d, J = 7.8 Hz), 7.73 (1H, d, J = 5.8 Hz), 7.68 (1H, s), 7.41 (2H, br. s), 4.66 (1H, br s), 2.85−2.77 (2H, m), 2.54 (2H, t, J = 10.4 Hz), 1.96−1.88 (2H, m), 1.45 (2H, br q, J = 9.1 Hz); LCMS (ES +ve) *m*/*z* 384.2 $(M + H)^+$; HRMS (ES +ve) *m*/*z* found 384.13742 $(M + H)^+$, calcd for $C_{20}H_{22}N_3O_3S$ 384.13764.

Compounds **16**, **18**−**21** were similarly prepared from the appropriate boronic acid or ester and **22**.

IKK-α and IKK-β Kinase Enzyme Assays. $pIC_{50} = -\log_{10} IC_{50}$, where the IC_{50} is the molar concentration of compound required to inhibit the kinase activity by 50%. IKK-β kinase inhibitory activity was determined using a time-resolved fluorescence resonance energy transfer (TR-FRET) assay. Recombinant human IKK-β (residues

Table 4. Kinase Inhibitory Potencies of **17**, **20**, and **21** (Values in pIC_{50})

compd	Akt1	B-Raf	EGFR	GSK3β	IKK-β	JNK3	Lck	MK2	p38α	Rock1
17	5.3	<5.0	<5.0	<4.6	7.0	<4.6	<4.6	<4.6	<4.6	5.9
20	<5.0	<5.0	<5.0	<4.6	6.9	<4.6	4.8	<4.6	<4.6	6.7
21	<5.0	<5.0	<5.0	<4.6	7.0	<4.6	4.7	<4.6	<4.6	6.1

1−737) was expressed in baculovirus as a C-terminal GST-tagged fusion protein. GST-IκBα substrate in a volume of 3 μL (25 nM final)/ATP (1 μM final) diluted in assay buffer (50 mM HEPES, 10 mM $MgCl_2$, 1 mM CHAPS, pH 7.4, with 1 mM DTT and 0.01% w/v BSA) was added to wells containing various concentrations of compound or DMSO vehicle (less than 5% final). The reaction mixture was initiated by the addition 3 μL of IKK-β (typically 0.5 nM final) in a total volume of 6 μL. The reaction was incubated for 15 min at room temperature, then terminated by the addition of stop reagent (3 μL) containing 50 mM EDTA and detection reagents in buffer (100 mM HEPES, pH 7.4, 150 mM NaCl, and 0.1% w/v BSA). Detection reagents comprise antiphosphoserine-IκBα-32/36 monoclonal antibody 12C2 (Cell Signalling Technology, Beverly, MA) labeled with W-1024 europium chelate (Perkin-Elmer, Beaconsfield, U.K.) and an allophycocyanin-labeled anti-GST antibody (Prozyme, San Leandro, CA). The mixture (9 μL total volume) was further incubated for at least 30 min at room temperature. The degree of phosphorylation of GST-IκBα was measured using a suitable time-resolved fluorimeter as a ratio of specific 665 nm energy transfer signal to reference europium 620 nm signal. IKK-α kinase inhibitory activity was determined in an analogous fashion, using 6-his-tagged full length IKK-α. Typical assay variability, as defined by measuring the pIC_{50} reproducibility of standard compounds [IKK-α, eight standard compounds with mean pIC_{50} values ranging from 5.4 to 7.2; IKK-β, seven standard compounds with mean pIC_{50} values ranging from 5.1 to 8.0], all run greater than 100 times in total, showed an average standard deviation around the measured pIC_{50} of ±0.2 log units for both assays.

Acknowledgment. We thank Duncan B. Judd and Bob Blade for assistance in the scale-up of **14**, Bill Leavens for HRMS analysis, and members of the Screening and Compound Profiling Departments based in Harlow, Essex, U.K., and Research Triangle Park, NC, for the generation of kinase inhibition data.

Supporting Information Available: Synthetic details and characterization data for **14**, **15**, **40**−**42**, and **23**−**39**; characterization data for **6**, **7**, **16**, **18**−**21**; LCMS traces for **17**, **20**, and **21**; experimental details for the PBMC and human whole blood assays. This material is available free of charge via the Internet at http://pubs.acs.org.

References

(1) Parang, K.; Sun, G. Design strategies for protein kinase inhibitors. *Curr. Opin. Drug Discovery Dev.* **2004**, *7*, 617–629.
(2) Häcker, H; Karin, M. Regulation and function of IKK and IKK-related kinases. *Sci. STKE* **2006**, *357*, re13.
(3) Karin, M.; Yamamoto, Y.; Wang, Q. M. The IKK NF-κB system: a treasure trove for drug development. *Nat. Rev. Drug Discovery* **2004**, *3*, 17–26.
(4) Bonizzi, G.; Karin, M. The two NF-kB activation pathways and their role in innate and adaptive immunity. *Trends Immunol.* **2004**, *25*, 280–288.
(5) Prajapati, S.; Tu, Z.; Yamamoto, Y.; Gaynor, R. B. IKKα regulates the mitotic phase of the cell cycle by modulating Aurora A phosphorylation. *Cell Cycle* **2006**, *5*, 2371–2380.
(6) Blazkova, H.; von Schubert, C.; Mikule, K.; Schwab, R.; Angliker, N.; Schmuckli-Maurer, J.; Fernandez, P. C.; Doxsey, S.; Dobbelaere, D. A. The IKK inhibitor BMS-345541 affects multiple mitotic cell cycle transitions. *Cell Cycle* **2007**, *6*, 2531–2540.
(7) Irelan, J. T.; Murphy, T. J.; DeJesus, P. D.; Teo, H.; Xu, D.; Gomez-Ferreria, M. A.; Zhou, Y.; Miraglia, L. J.; Rines, D. R.; Verma, I. M.; Sharp, D. J.; Tergaonkar, V. A role for IκB kinase 2 in bipolar spindle assembly. *Proc. Natl. Acad. Sci. U.S.A.* **2007**, *104*, 16940–16945.
(8) Coish, P. D. G.; Wickens, P. L.; Lowinger, T. B. Small molecule inhibitors of IKK kinase activity. *Expert Opin. Ther. Pat.* **2006**, *16*, 1–12.
(9) Christopher, J. A.; Avitabile, B. G.; Bamborough, P.; Champigny, A. C.; Cutler, G. J.; Dyos, S. L.; Grace, K. G.; Kerns, J. K.; Kitson, J. D.; Mellor, G. W.; Morey, J. V.; Morse, M. A.; O'Malley, C. F.; Patel, C. B.; Probst, N.; Rumsey, W.; Smith, C. A.; Wilson, M. J. The discovery of 2-amino-3,5-diarylbenzamide inhibitors of IKK-α and IKK-β kinases. *Bioorg. Med. Chem. Lett.* **2007**, *17*, 3972–3977.
(10) Reagent selection, filtering, and array enumeration were carried out using proprietary software based on the Daylight toolkit (www.daylight.com). The starting point was a list of available aryl bromides or iodides from the corporate collection or from external suppliers. These were filtered to remove certain defined functionalities that are potentially unstable or undesirable. Substructure searches were used to exclude compounds containing more than one aryl halide or any boronic acid, sulfonyl halide, aldehyde, acid chloride, β-keto ester, thiol, anhydride, isothiocyanate, or epoxide. Compounds containing over 25 heavy atoms were also excluded. Approximately 8000 aryl halides remained.
(11) The 3D aryl halide database was built and searched and the pharmacophore built using Catalyst (Accelrys Inc., www.accelrys.com). Fast conformer generation was used with a maximum of 50 conformers per molecule. The standard H-bond acceptor function was modified to include only strong, neutral, planar H-bonding groups, and excluded volume spheres were placed with reference to the homology model. Docking studies into the homology model (see ref 9) were performed using version 3.0 of Gold (Cambridge Crystallographic Data Centre, www.ccdc.cam.ac.uk). Assessment of docking scores and binding modes was carried out visually, using a combination of software including the Spotfire Decision Site (spotfire.tibco.com) interfaced with Accelrys Viewer Pro using proprietary code.
(12) Hass, H. B.; Bender, M. L. Reaction of benzyl halides with the sodium salt of 2-nitropropane. A general synthesis of substituted benzaldehydes. *J. Am. Chem. Soc.* **1949**, *71*, 1767–1769.

JM9000117